

Article

Deformation Analysis and Reinforcement Effect of Tunnel Pile Excavation of a Subway Station in a Weak Stratum

Jianbing Lv , Jianjun Lu, Jingkai Huang, Juan Huang * , Jia Li and Xiangyang Ge

School of Civil and Transportation Engineering, Guangdong University of Technology, Guangzhou 510006, China; ljb@gdut.edu.cn (J.L.)

* Correspondence: cvjuanhuang@gdut.edu.cn; Tel.: +86-139-2628-8216

Abstract: The underground hole pile excavation method causes a large vertical displacement in a weak stratum, which affects the safety of structures. For the first time, the hole pile excavation method is being used to construct a subway station in South China, and the settlement law of the area is not clear. It is important to clarify the deformation law of the hole pile excavation method in weak strata and the effect achieved by appropriate reinforcement measures. In this paper, by establishing a three-dimensional finite element model of the structure–soil contact element and combining it with the field monitoring data, the law of surface settlement caused by the hole pile excavation method with different thicknesses of the weak stratum has been studied. In order to improve the stability of the surrounding rock and reduce the vertical deformation of the surface, the Metro Jet System (MJS) is used to form inclined piles in the area of large surface deformation, and the effect after reinforcement was evaluated. The results show that as the weak layer thickness ratio increases, the surface settlement also increases. In the case of no reinforcement, a vertical settlement of 116 mm can be achieved when the thickness of the weak layer is 14 m. The vault of the tunnel is in the weak layer and the deformation is obvious. When the vault is not in the weak layer, the settlement is obviously reduced. After MJS pile reinforcement, under the action of soil extrusion, the self-stability of the surrounding rock is strengthened, and the oblique jet grouted pile forms a stable ‘triangle’. The vertical settlement value is basically stable at around 30 mm, which meets the requirements of the regulations. If the tunnel is not reinforced, the self-stability of the surrounding rock above the tunnel arch is poor and the maximum settlement is at the surface. After MJS reinforcement, the maximum settlement is at the vault. The vertical settlement of the ground surface can be effectively controlled by using the MJS pile forming technology in the middle of the tunnel pile driving method.

Keywords: tunneling; pile excavation method; weak stratum; MJS method; structure–soil interaction



Citation: Lv, J.; Lu, J.; Huang, J.; Huang, J.; Li, J.; Ge, X. Deformation Analysis and Reinforcement Effect of Tunnel Pile Excavation of a Subway Station in a Weak Stratum. *Buildings* **2023**, *13*, 1943. <https://doi.org/10.3390/buildings13081943>

Academic Editor: Yong Tan

Received: 27 June 2023

Revised: 11 July 2023

Accepted: 28 July 2023

Published: 30 July 2023



Copyright: © 2023 by the authors. Licensee MDPI, Basel, Switzerland. This article is an open access article distributed under the terms and conditions of the Creative Commons Attribution (CC BY) license (<https://creativecommons.org/licenses/by/4.0/>).

1. Introduction

As urbanization continues, the influx of large numbers of people into the city has led to traffic congestion [1]. Rail transit can better solve the problem of traffic congestion and provide residents with fast and convenient travel due to its barrier-free underground passage [2,3]. Subway construction is mainly based on the cut-and-cover method and the undercutting methods. Compared with the undercutting method, the open cut method does not require much consideration of geological conditions, but it does require excavation of the road, which disrupts traffic. Especially for the main roads of megacities, it seriously affects the travel of citizens and even interferes with the operation of the city. In the city center, to build subway stations, most cities still use the underground excavation method. In China, Turkey, Vietnam, the United States, Denmark and other countries, there are a large number of soft strata in coastal areas, and since most of the urban rail transit is underground, the concealed subway station is inevitably built in the soft strata [4,5]. As a special geological environment, the weak layer has a low quality of the surrounding rock. After tunnel excavation, the stress released by the free face is relatively large, which easily

causes the structure to settle, affecting the tunnel under construction and the surrounding environment [6,7]. Every year, the number of surface landslides caused by underground excavation and construction of underground projects around the world is large, which seriously affects traffic safety and the safety of people's lives and property. Therefore, the construction of subway station by an underground excavation method must strictly control the surface subsidence to prevent collapse. The hole pile excavation method has relatively high settlement requirements. From the existing research, it can be known that the construction of the pilot tunnel and the arch structure are the main causes of settlement [8]. It is particularly important to study the influence of the depth of the weak layer on the surface settlement of the underground pile-face method.

The high-pressure jet grouting method can be considered for the reinforcement of tunnel-surrounding rocks with poor stability [9,10]. The traditional high-pressure rotary jet grouting method will have a large squeezing effect on the surrounding area during the construction process, causing ground uplift, surface cracking, etc., which will affect the normal use of surrounding buildings and municipal pipelines, and even cause more serious damage [11]. Anchor reinforcement and pipe roof reinforcement can play a role in some projects, but they are slightly inferior to those in areas with large soft strata. Based on the high-pressure rotary jet grouting method, an all-round high pressure rotary jet grouting method, known as MJS, has been developed [12,13]. The unique porous pipe and front-end positive suction device are used to realize positive grouting in the borehole and pressure monitoring in the ground. By using this technology, the slurry discharge can be adjusted, the ground pressure can be effectively controlled, the ground pressure condition can be stabilized, the surface settlement can be reduced, and the environmental impact can be greatly reduced. Compared with the traditional jet grouting technology, this technology is more advanced and environmentally friendly, which can significantly ensure the pile diameter and engineering safety.

Due to its complex mechanical conversion system [14], the excavation area of an underground subway station is relatively large. Historically, it has been difficult to construct subway stations using concealed piles in soft ground due to economic and technical constraints. With the development of the economy and the improvement of technology, the technology of underground pile driving in soft ground has gradually been applied to the construction of subway stations. However, it often causes relatively large surface subsidence, which requires repeated grouting reinforcement, which easily delays construction progress, but also causes layer instability and increases risks. Based on the data of field monitoring, the horizontal MJS grouting method [15,16] can effectively control the settlement of a soft soil tunnel, achieve the effect of strengthening the foundation, and reduce the surface uplift caused by grouting to achieve the effect of micro-disturbance. The MJS pile can also be used to reinforce the weak foundation in the vertical direction to improve the bearing capacity of the foundation [17]. The MJS grouting method does not require a large area, and it can also be used to reinforce the foundation in a narrow space, such as when the shield tunnel passes through the pedestrian passage and the bridge pile [18]. The MJS grouting method can also be used in karst areas to avoid the influence of ground movement of adjacent piles caused by deep excavation [13]. The tunnel pile driving method does not need to destroy the road surface and does not affect the construction technology of traffic operation [19]. Taking advantage of the MJS method, which can be grouted at any angle, the surface settlement caused by the tunnel pile excavation subway is grouted and reinforced, and then the tunnel soil is excavated to reduce the stress loss and control the surface settlement.

The development of computers has been helpful in solving the non-linear problem of tunnelling, and the numerical approximate solution of the partial differential equation can be solved by powerful computing power [20,21]. The maximum vertical displacement of existing adjacent tunnels is analyzed using the finite element principle [22]. Finite element numerical simulation is used to study the settlement control problem caused by excavation of the tunnel arch structure [23]. MJS grouted reinforcement forms piles. The contact area

between the soil and the pile is relatively large. When the soil moves, relative displacement occurs. At this time, the structure–soil contact must be considered. The structure–soil contact problem is a very complex, non-linear problem, but the finite element analysis software can solve the pile–soil and structure–soil contact problems [24,25].

MJS pile-forming technology is most commonly used for vertical or horizontal foundation reinforcement. For the section with large settlements, the original method of large tubular sheathing and grouting cannot reinforce the strength of the surrounding rock. In the first construction stage of the bored pile method, the construction of the pilot tunnel causes large settlements. Therefore, this paper explores the use of the MJS method to reinforce the foundation and establishes a nonlinear finite element model considering the structure–soil contact, and comprehensively evaluates the effect of MJS pile reinforcement. At the same time, the influence of different thicknesses of the weak layer on the surface settlement is also analyzed, which lays the foundation and accumulates experience for the promotion of the cavity pile concealed excavation method in South China, and even in countries or regions around the world where there are soft soil areas.

2. Engineering Case

2.1. Engineering Overview and Difficulties

The metro station under construction is located on the busy Guangzhou Dongfeng Road, and a large number of pipelines are buried under the road. In order to avoid disruption of traffic and pipeline relocation, the construction unit clearly adopts the hole pile method in the feasibility analysis report. Before the construction of the hole pile method, the first step is to excavate the vertical shaft, similar to the foundation pit, vertically and on the road surface. After reaching the specified height, the horizontal trench is excavated vertically and on the cross section of the road, and then the underground station is excavated horizontally with the road. The first step in the hole pile method is to excavate the pilot tunnel and construct the lining. In this case, it is a hole pile method with three pilot tunnels and double arches. The second step is to construct side piles and steel pipe piles in the pilot tunnel; the third step is to construct two vaults to form a stable pile-beam-arch frame structure in the tunnel to protect a large area of the excavation. The fourth step is to excavate the negative second floor of the station and construct the side wall, central slab, and floor slab, as shown in Figure 1. However, due to the variable complexity of the geology in South China, the station is located in the thick section of the weak layer during the construction process. The surface settlement caused by the excavation is relatively large and requires continuous grouting reinforcement, which seriously affects the construction progress and even causes safety accidents. Above the underground excavation station is a normal road, which cannot be completely closed during construction.

2.2. Geological Engineering Condition

The stratigraphy of the subway station is not uniform from east to west, and the thickness of the weak layer gradually increases, leading to an increase in unstable factors. The soil layers from top to bottom are plain fill, plastic residual soil, heavily weathered siltstone, and lightly weathered conglomerate, with alternating hard plastic residual soil and fully weathered clastic rock. The stratigraphic section is shown in Figure 2. Due to the uneven distribution of the strata, some of the pilot tunnels are located in the plastic residual soil, resulting in a relatively large settlement of the pilot tunnel excavation to the east. The plastic residual soil is brownish red and other colors. It is wet and plastic. It is mainly composed of silt and clay particles. It is an argillaceous siltstone weathered residual soil. There are many fine sand particles and a small amount of weathered rock debris that easily softens and disintegrates in water. The residual soil after the excavation of the pilot tunnel releases a lot of stress, and the weather in southern China is hot, humid, and rainy, which accelerates the softening and disintegration of the soil, resulting in a sharp increase in surface subsidence.

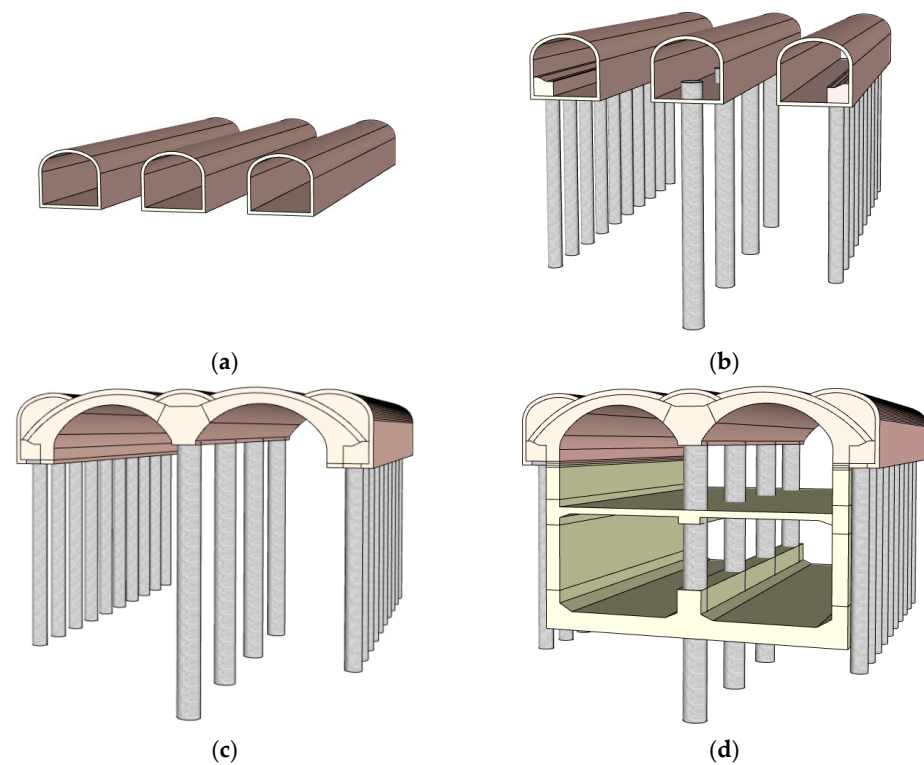


Figure 1. Construction flow chart: (a) The pilot tunnel; (b) Pile beam; (c) The top arch; (d) Main body.

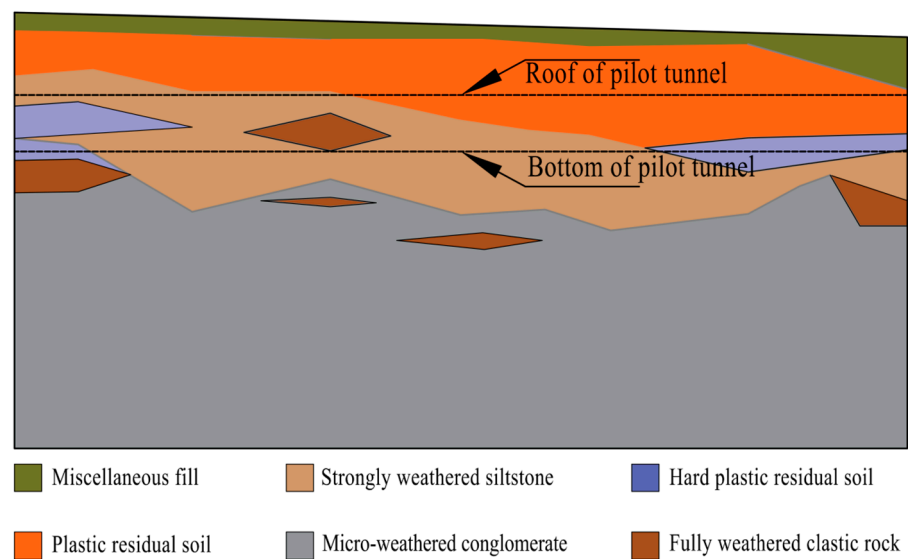


Figure 2. Geological distribution map.

2.3. Research Case

The underground station is a shallowly buried station that is basically at the same level. However, due to the uneven burial depth of the plastic residual soil, it shows a state of thickness in the east and thinness in the west. Therefore, it is convenient to study the settlement law of the underground excavation hole pile method in different weak layer thicknesses. The layer is divided into five working conditions, and the corresponding residual soil thicknesses are 6 m (Case 1), 8 m (Case 2), 10 m (Case 3), 12 m (Case 4), and 14 m (Case 5), and the length of each working condition is about 30 m. The corresponding five working conditions are used to construct a three-dimensional model by using the finite element analysis software GTS NX, and the settlement law before reinforcement and the settlement control effect after MJS reinforcement are analyzed.

2.4. Reinforcement Scheme

In the actual monitoring, it is found that the surface settlement of the section with the largest residual soil thickness reaches 102 mm, far exceeding the warning control value of 40 mm [26]. After finding the early warning, the construction unit immediately adopts a series of measures such as grouting reinforcement, small pipe reinforcement, and anchor reinforcement to reinforce the layer, which increases the investment of manpower and material resources and also affects the construction time. The upper part of the bored pile method is a normal driving road, so the whole section cannot be closed for reinforcement, so the traditional high-pressure jet grouting pile cannot be used for foundation treatment.

There are many high-rise buildings in the vicinity of the station, and foundation strengthening is carried out in dense building clusters. A foundation strengthening method with micro-disturbance and strong controllability is urgently needed. With the improvement of technology, the MJS method based on high-pressure jet grouting technology was developed. During the construction process, when the pressure in the hole measured by the pressure sensor is high, the opening size of the suction hole can be controlled by the oil pressure connection, so as to adjust the mud discharge amount to control the pressure value range in the ground. It greatly reduces the impact on the environment and avoids the squeezing effect, which greatly reduces the occurrence of surface deformation, building cracking, and structural displacement during construction. MJS can realize grouting reinforcement at any angle, with a small floor area and large pile diameter. The general reinforcement plan of the MJS method is to grout the piles from the middle of the road. The expected diameter of the piles on both sides is 2 m, and the expected diameter of the middle pile is 1.5 m, so that a stable triangular reinforcement area is formed above the guide hole, as shown in Figure 3.

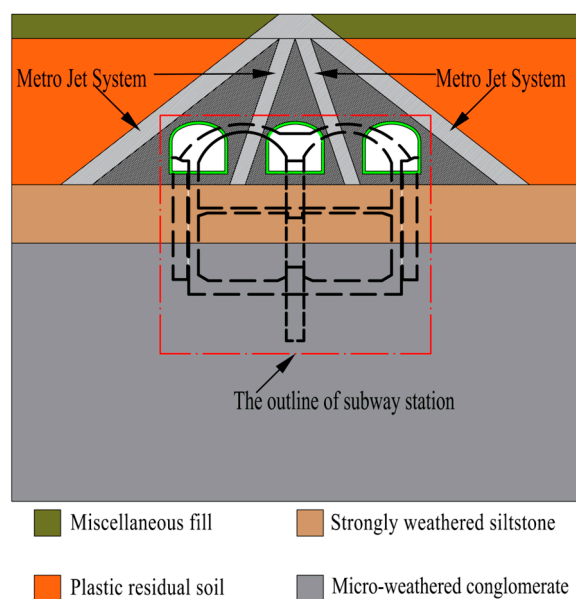


Figure 3. Reinforcement diagram.

3. MJS Pile Diameter

The diameter of an MJS pile is an important design index of engineering. The diameter calculation method of MJS pile foundation is introduced as the pile diameter of three-dimensional finite element model.

3.1. Circular Free Turbulence Theory

Jet theory is the basis of the jet breaking mechanism, and high-pressure jet grouting is a turbulent jet. In practice, the boundary between the jet and the surrounding fluid is not obvious. To simplify the calculation model, the jet is usually divided into the

initial and main sections according to the flow characteristics, and the transition section is ignored. x represents the axial coordinate calculated from the jet source point, and r is the radial coordinate perpendicular to the x -axis, as shown in Figure 4. The high-pressure jet grout is sprayed from a small-diameter nozzle through a high-pressure pump to collect the enormous energy of the liquid, forming a high-speed jet flow and cutting the surrounding soil.

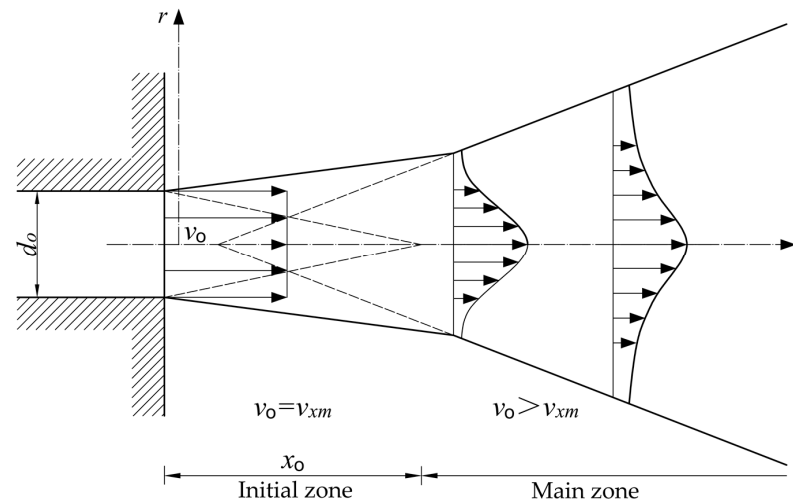


Figure 4. Diagram of turbulent jet region of circular segment.

3.2. MJS Pile Diameter Derivation

In the similarity analysis of the jet, the velocity on the axis of the starting section ($x > x_0$) is constant as the initial velocity (v_0). The boundary of the jet in the main section expands linearly, and the maximum axial time-averaged velocity (v_{xm}) decays with the first power ($1/x$) of x , that is:

$$\frac{v_{xm}}{v_0} = \alpha \frac{d_0}{x} \quad (1)$$

where v_0 is the exit velocity of shotcrete, α is a dimensionless factor quantifying interaction between jet and surrounding fluid [27], d_0 is the diameter of the nozzle, and x is the distance of the stroke of the spray liquid.

The maximum velocity at the center of the axis can be derived:

$$v_{xm} = \frac{\alpha d_0 v_0}{x} \quad (2)$$

The impact force generated by the slurry from the nozzle hitting the surrounding soil with a high-pressure jet can be divided into stagnation pressure and water hammer pressure. The generation of water hammer pressure is related to the inertia and compressibility of the fluid. The soil is a kind of incomplete elastic body with discrete characteristics. It is easily damaged after being hit by the slurry, which buffers the water hammer pressure of the jet. Generally, only the stagnation pressure is considered [28] and can be calculated by the following formula:

$$P = \frac{\rho v_{xm}^2}{2} \quad (3)$$

and since MJS is a triple-fluid jet grouting method, the liquid for punching and cutting the soil is water, so ρ is the density of water.

The impact force will decay with the increase in r , and the velocity on the center line is the largest. Bringing (2) into (4) we obtain the maximum jet impact force:

$$P_m = \frac{\rho \alpha^2 d_0^2 v_0^2}{2x^2} \quad (4)$$

The initial speed can be calculated using the following formula:

$$v_0 = \sqrt{\frac{2P_j}{\rho}} \quad (5)$$

where P_j is the injection pressure.

The impact force on the beam axis decreases with the increase in P_m . When it decreases to the maximum resistance F of the soil, the failure area of the soil reaches the limit, and the corresponding x is the limit cutting distance x_l .

For cohesive soil, the theoretical formula proposed by Ho [29] can be used to calculate the soil resistance:

$$F = 2.4S_u \quad (6)$$

Flora [27] and Shen [30] derived the decay coefficient as:

$$\alpha = \left(1 + 0.054 \frac{P_a}{P_{atm}}\right) \alpha_w \quad (7)$$

where p_a = pressure of the injected air (between 0.5 and 1.5 MPa), p_{atm} = atmospheric pressure (100 kPa), and α_w is equal to 16 [31].

Let $P_m = F$,

$$x_l = \alpha d_0 v_0 \sqrt{\frac{\rho}{4.8S_u}} \quad (8)$$

where S_u is the undrained shear strength of cohesive soil; there is no correlation between pile radius and slurry density.

Therefore, the diameter D of the MJS pile can be expressed as:

$$D = d_0 + 2x_l \quad (9)$$

4. Field Monitoring and Finite Element Analysis

4.1. Location of Monitoring Points

In order to ensure the safety of the small pilot tunnel and the main body and the surrounding area during the construction process and to guide the construction correctly, it is necessary to monitor the small pilot tunnel and the main body enclosure structure and the surrounding area. According to the specification [26], a monitoring point is set up every 15 m in the longitudinal direction of the road surface above the tunnel, and a monitoring point is also set up every 10 m in the transverse direction. The level will be used to monitor daily changes in surface settlement. DC11 is the first monitoring point, DC20 is the tenth monitoring point, and 01–05 is the horizontal monitoring point. The monitoring layout is shown in Figure 5.

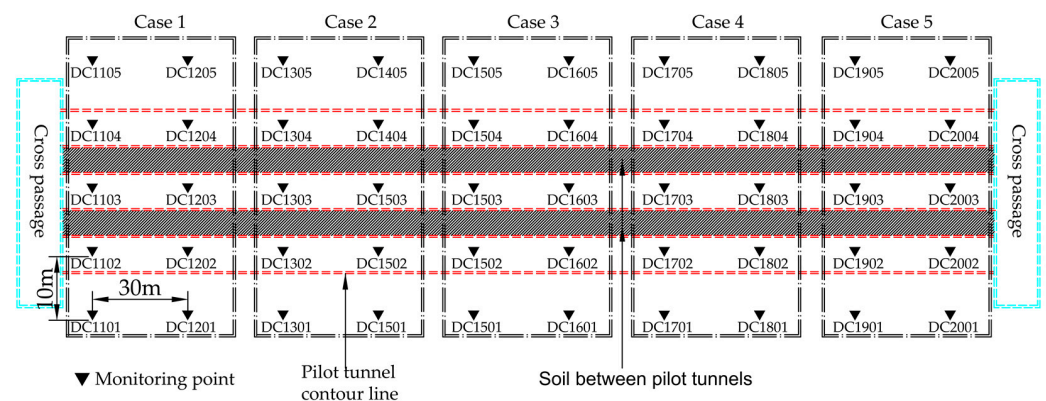


Figure 5. Layout diagram of monitoring plane.

4.2. Finite Element Model

The finite element analysis software GTS NX is used to construct a three-dimensional finite element model. The layer structure method is used to study the settlement law of the underground pile driving method in uneven layers and to evaluate the effect of the MJS method on surface settlement control. In the theory of geomechanics, when the grid size is six times the excavation diameter, the calculation error is small. Therefore, the size of the finite element three-dimensional model X is 150 m, Y is 30 m, and Z is 50 m, as shown in Figure 6.

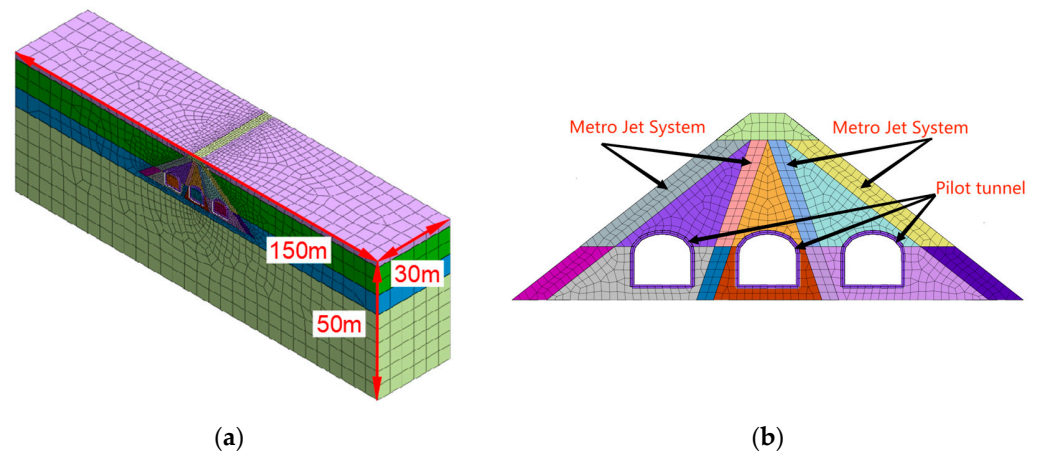


Figure 6. Finite element model diagram. (a) Schematic of the stratigraphic structure method; (b) MJS method pile schematic diagram.

In this paper, only the effect of MJS piles on surface settlement control in the excavation of concealed cavity piles is investigated, and the modeling process of MJS pile refinement is not considered at present. Therefore, in the finite element model, the MJS pile is numerically simulated by activating the unit in segments and changing the unit properties, and the tunnel excavation is carried out after the MJS pile is loaded. The preliminary parameters of MJS are: $P_j = 40$ MPa, the density of the injection fluid is taken as the density of water $\rho = 1000$ kN/m³, the undrained shear strength of soft soil $S_u = 50$ kPa measured at the construction site, the nozzle diameter $d_0 = 25$ mm, and the injection air pressure $p_{atm} = 0.65$ MPa. The diameter of the MJS pile can be initially calculated by Equation (9). Bringing (5)–(8) into (9) we obtain:

$$\begin{aligned}
 D &= d_0 \left[1 + 2\alpha_w \left(1 + 0.054 \frac{P_j}{p_{atm}} \right) \sqrt{\frac{2P_j}{4.8S_u}} \right] \\
 &= 0.025 \times \left[1 + 2 \times 16 \times \left(1 + 0.054 \times \frac{650}{100} \right) \times \sqrt{\frac{2 \times 40 \times 10^6}{4.8 \times 50 \times 10^3}} \right] = 1.976(\text{m})
 \end{aligned} \quad (10)$$

In the finite element model, the diameter of the MJS pile was set to 2 m. To match the tunnel excavation process, the diameter of the inner MJS pile was set to 1.5 m by changing the grouting parameters. The effect of the cement setting process of the MJS piles was not considered, and the construction phase of the MJS was set to zero for displacement prior to tunnel excavation.

4.2.1. Basic Assumptions and Boundary Conditions

Basic assumptions:

- (1) Field groundwater is not abundant, so the finite element analysis ignores the infiltration of groundwater;
- (2) Uniform horizontal distribution between soil layers;
- (3) Materials are isotropic and homogeneous;

- (4) The modified Mohr–Coulomb constitutive is used for soil, and the elastic constitutive is used for concrete;
- (5) The time effect of concrete from initial setting to expected strength is not considered;
- (6) Soil–structure interaction is considered.

Contact Element:

In GTS NX software, the structure–soil interaction is composed of a solid element and a contact element, and the contact element represents the contact relationship between pile and soil. The contact element consists of tangential spring and normal spring stiffnesses. The values of the normal stiffness modulus K_n and tangential stiffness modulus K_t can be automatically calculated by the three-dimensional model in GTS NX software.

Boundary Conditions:

The top nodes of the model are free and do not impose any constraints. The bottom nodes apply vertical constraints and the surrounding nodes apply horizontal constraints.

4.2.2. Finite Element Parameters

The geological prospecting report is simplified to one layer, and the soil types from top to bottom are: miscellaneous fill, plastic residual soil, highly weathered siltstone, and conglomerate. The pile diameter of the MJS pile is calculated using the derived Formula (10). The soil material parameters obtained from the field and laboratory test data are shown in Table 1.

Table 1. Mechanical parameter table.

Structure	Parameter	Cohesion (Mpa)	Poisson's Ratio	Volumetric Weight (kN/m ³)	Internal Friction Angle (β)	E_{50}^{ref} (MPa)	E_{oed}^{ref} (MPa)	E_{fur}^{re} (MPa)	E (MPa)
miscellaneous fill		0.010	0.35	21	10	4.16	3.28	26.06	\
plastic residual soil		0.023	0.4	24	18	7.02	5.85	40.95	\
highly weathered siltstone		0.045	0.3	25	25	12.96	10.8	75.6	\
conglomerate		\	0.3	27	40	\	\	\	6000
C25 lining		\	0.2	25	\	\	\	\	30,000
MJS		\	0.2	25	\	\	\	\	400

E_{50}^{ref} , secant elastic modulus in shear hardening; E_{oed}^{ref} , secant elastic modulus in shear hardening; E_{fur}^{re} elastic modulus at unloading; E, elastic modulus.

4.2.3. Simulation of Construction Stage

In the study of the existing hole pile method [8,32], it was found that the excavation of the guide hole was the main construction stage that caused the surface settlement. Controlling the settlement of the guide hole is conducive to controlling the settlement of the subsequent construction process. Therefore, the working conditions of the stage in this study include the excavation construction simulation of the guide hole of the hole pile excavation method and the construction simulation of the MJS pile. The birth and death element method is used to simulate the excavation process, and the construction process of the MJS pile is simulated by changing the element properties. The specific construction steps are as follows:

- (1) Initial stress field (activate soil, load, and boundary conditions and set deformation clearing);
- (2) MJS pile reinforcement treatment simulation (study of the reinforcement effect) in which a total of two kinds of MJS pile are set up, with an outer diameter of 2 m and an inner diameter of 1.5 m;
- (3) Pilot hole excavation simulation (excavation according to the site construction plan, digging 1 m per day) starting with the first pilot hole excavation, followed by the right pilot hole excavation, and finally the left pilot hole excavation, a total of 45 construction steps.

5. Results Analysis

5.1. Field Monitoring Results

5.1.1. Longitudinal Settlement Analysis

In the process of tunnel excavation, it can be known from the Peck curve that the settlement value of the observation point in the middle of the tunnel is the largest. Therefore, DC1003–DC1203, DC1203–DC1403, DC1403–DC1603, DC1603–DC1803, and DC1803–DC2003 are adopted, corresponding to the plastic residual soil (soft soil layer) thickness of 6 (Case 1), 8 (Case 2), 10 (Case 3), 12 (Case 4) and 14 (Case 5) meters. According to the actual construction schedule of digging 1 m per day, the middle pilot tunnel is excavated first, then the right pilot tunnel is excavated, and finally the left pilot tunnel is excavated. Each working condition lasts for 90 days. The monitoring data in Figure 6 show that the records start 30 m west of each monitoring point. It can be seen from Figure 7 that the thicker the plastic residual soil is, the greater the surface settlement caused by tunnel excavation. When the thickness of the weak layer is 14 m, the diffusion range of settlement is expanded. During the excavation of the middle pilot tunnel, the settlement growth rate is large, while the settlement rate of the left and right pilot tunnels is moderate, and the settlement is mainly concentrated in the excavation process of the middle pilot tunnel. In the soft layer, after the first stress release, the settlement caused by the second stress release is greatly weakened, so it is necessary to focus on the reinforcement of the middle pilot hole.

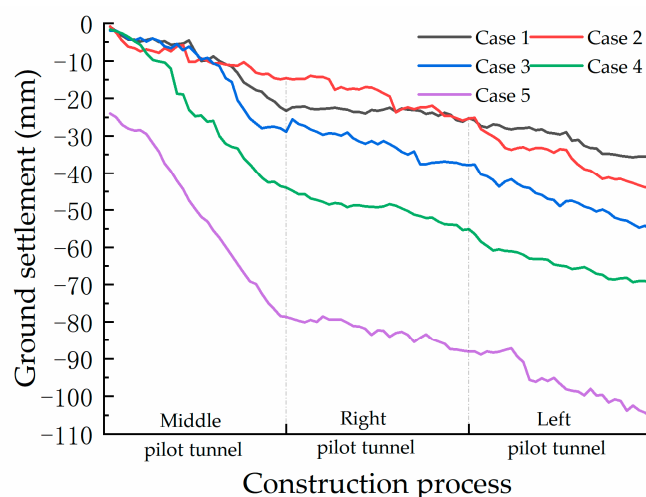


Figure 7. Cumulative value of longitudinal settlement.

5.1.2. Lateral Settlement Analysis

From the lateral settlement distribution map in Figure 8, it can be seen that the lateral settlement in the weak stratum basically corresponds to the Peck curve distribution, with large settlement in the center and small settlement on both sides. The closer to the center of the tunnel, the faster the settlement rate. The buried depth of the tunnel is basically the same, so the inflection point of each working condition appears about 10 m away from the center of the tunnel. When the thickness of the weak stratum is 14 m, the whole section of the pilot tunnel is in the weak stratum, and the bearing stratum of the tunnel cannot provide sufficient bearing capacity, which makes the surface settlement of this working condition more serious and the settlement amount increases rapidly. If the whole tunnel section is in a weak stratum without reinforcement, it is not recommended to excavate the tunnel.

5.2. Comparative Analysis of Monitoring and Simulation Data

Using the finite element software GTS NX, the construction process of the small pilot tunnel is simulated by the finite element construction stage, and the change of the surface settlement law is calculated, as shown in Figure 9. A total of five working conditions are set

up, each with a length of 30 m. The small number is the observation point, that is, the change trend of the settlement process after excavation. The large number is another observation point, that is, the change trend of the settlement process 30 m from the excavation face. With the increase in the thickness of the soft soil layer, both the simulated value and the observation value of the surface settlement value show an increase, and the increasing trend of the surface is gradually accelerated. It can be seen from Figure 9 that the front observation point of each working condition shows that the settlement rate is continuously weakened, and it first increases sharply and then gradually converges. Each time a large settlement is generated, it is the first step in the excavation of the pilot tunnel. The settlement rate of the rear observation point continues to increase, first slowly and then rapidly. The settlement is mainly concentrated in the construction stage of the middle pilot tunnel, which is about 2/3 of the total settlement value. When the thickness of the weak layer exceeds 8 m (Figure 10a), the tunnel vault is under the weak layer, and the surface settlement does not exceed the threshold value, which is within the controllable range. When the thickness of the weak layer is 12 m (Figure 10b), the tunnel is in the weak layer and the surface settlement value is about two times the threshold value. When the thickness of the weak layer is 14 m (Figure 10c), the whole guide tunnel is in the weak layer, and the surface settlement value is about three times the threshold value.

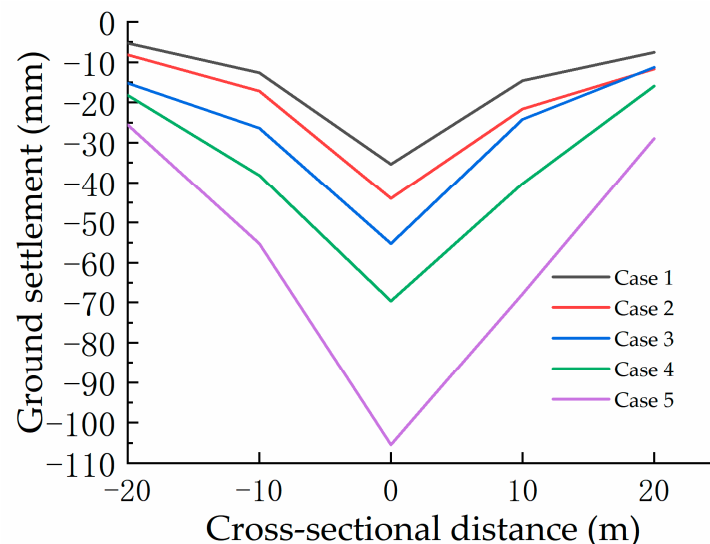


Figure 8. Transverse settlement distribution map.

Overall, the greater the thickness of the weak layer, the more accurate the simulated value and the measured value. The relatively large relative errors between the monitoring values and the simulation of operating conditions 1, 2, and 3 are due to the assumptions. In the finite element simulation, the layer is too simplified. In the actual field, the layer varies greatly in the cross section, and there are still areas of good geological conditions that are considered weak layers in the simulation. As a result, the properties of the formation changed in the simulation, resulting in a large error. The monitoring values of working conditions 3 and 4 are relatively close to the simulated values. This is because the actual engineering and simulated soil properties are relatively familiar, so the error is relatively small. However, no matter what kind of working condition, it can be seen from Figure 9 that the change trend of simulated value and measured value is about the same. After the large settlement caused by the excavation of the middle pilot tunnel, the settlement of the excavation of the following two pilot tunnels is significantly alleviated, both of which indicate that the excavation of the middle pilot tunnel is the main construction stage leading to settlement.

The results of the finite element simulation were verified by the field monitoring data. Although there are errors in the monitoring data, the error range is reasonable, and the

accuracy of the finite element model can be basically determined. It provides authenticity and accuracy for the effect of surface settlement control of the MJS pile reinforced concealed hole pile method in soft ground below.

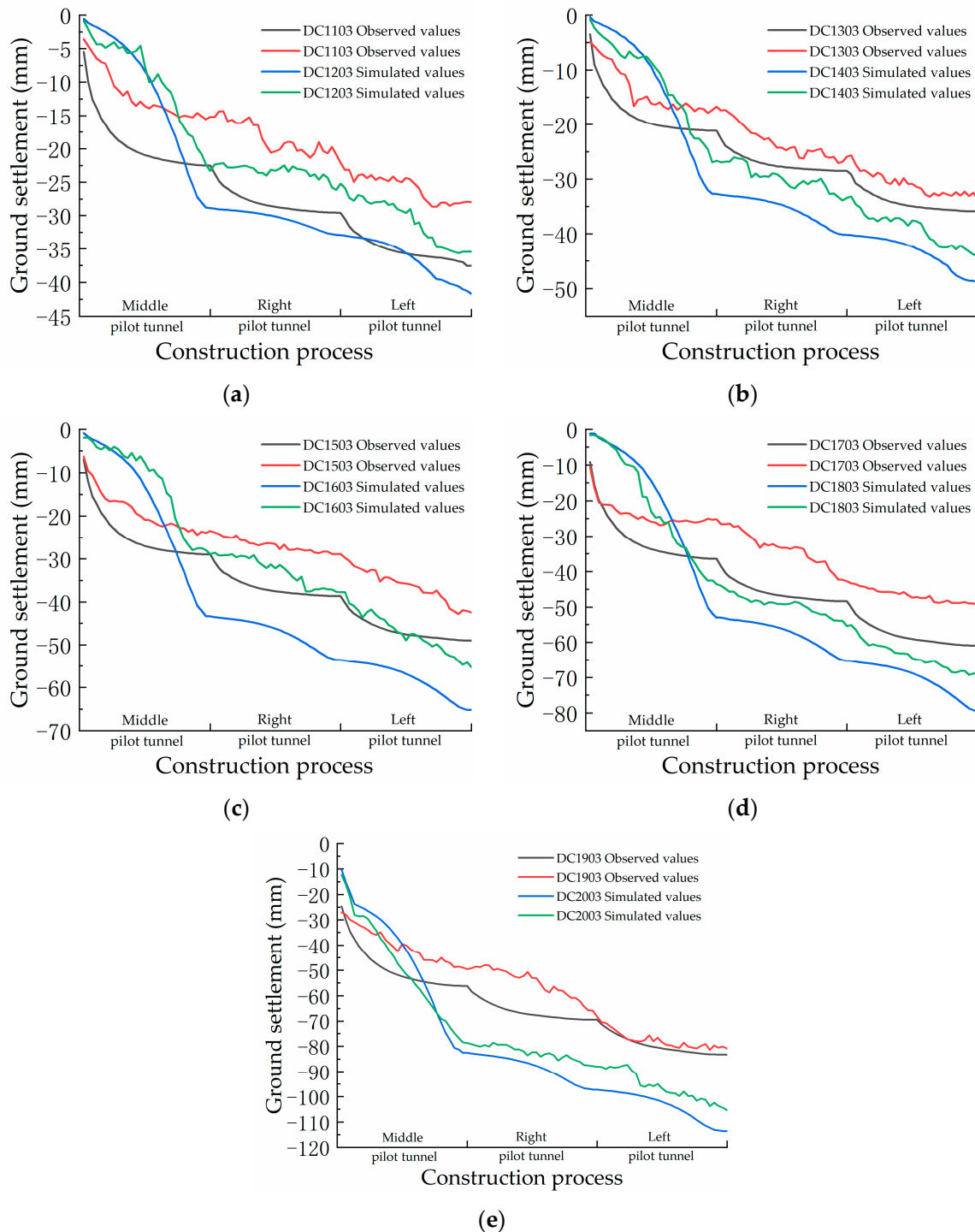


Figure 9. Ground surface settlement laws: (a) Case 1; (b) Case 2; (c) Case 3; (d) Case 4; (e) Case 5.

Tunnel excavation has caused excessive settlement of the urban surface, which will endanger the operation of the whole city. Therefore, for the excessive settlement caused by excavation, this paper explores the use of the MJS method to pile foundation treatment in advance, before carrying out tunnel excavation to ensure that the settlement value is controlled within a reasonable range.

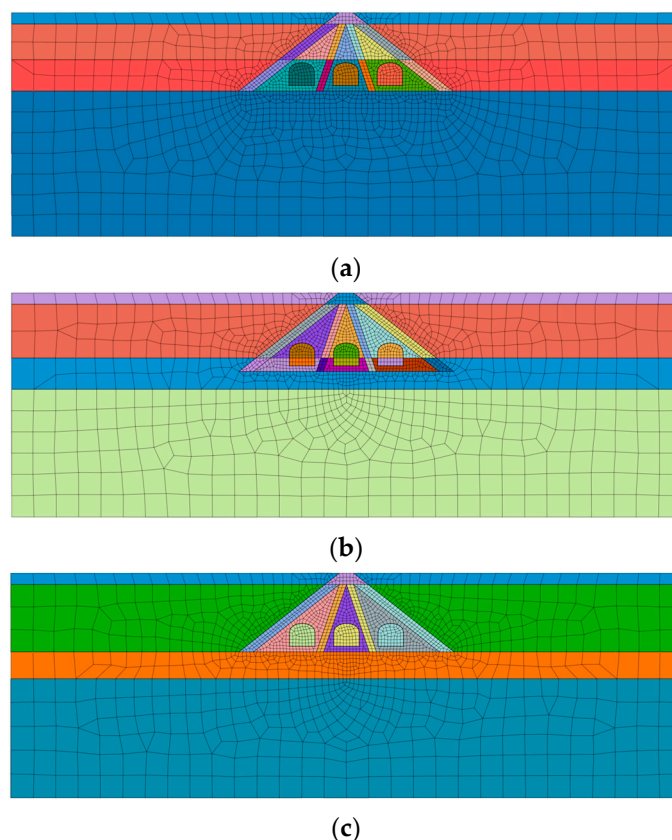


Figure 10. Typical section diagram: (a) Case 1; (b) Case 3; (c) Case 5.

5.3. MJS Method Pile Reinforcement Effect

In Section 5.2, the measured data and simulated data are compared to prove the rationality of the finite element model. Under the condition that other conditions remain unchanged, the finite element simulation of the settlement foundation reinforcement of the hole pile method is carried out by using the pile diameter of the MJS pile derived from the Formula (10), and the reinforcement effect is now evaluated.

5.3.1. Longitudinal Soil Settlement

In Figure 9a, the settlement value caused by the excavation of the hole pile method in working condition 1 does not exceed the threshold value, so it is not necessary to reinforce the foundation. The oblique jet finite element reinforcement model of the MJS method is carried out for working Case 2, 3, 4 and 5. In Figures 11 and 12 and Table 2, the most severe surface settlement in working Case 5 can reach 116 mm. After MJS pile reinforcement, the surface settlement is effectively suppressed so that the final surface settlement value is 34 mm, which is reduced by 70%. In other working conditions, the settlement of more than 50% is also reduced by MJS pile reinforcement, which is below the threshold of 40 mm. The soil after reinforcement can be excavated in the next step. The maximum value of unreinforced settlement appears on the surface, and the maximum value appears on the vault of the left and right guide holes after MJS reinforcement.

Figure 11a–c shows the settlement analysis of the center guide hole, right guide hole, and left guide hole vault selected from the rear observation point. From Figure 11a–c, it can be seen that the surface settlement becomes obvious when each pilot tunnel is excavated, and the increment is large, indicating that the mutual disturbance of each pilot tunnel excavation is not obvious. This is because the MJS method divides the three pilot tunnels into the upper area, so that the three pilot tunnels do not cause too much disturbance when they are excavated separately. At the same time, the MJS pile forms a stable triangular structure above the pilot tunnel, which is conducive to reducing formation loss and con-

trolling deformation. This is because the MJS method can control the opening size of the suction hole through the oil pressure joint when the pressure in the hole measured by the pressure sensor is high, so as to adjust the mud discharge amount to control the pressure value range in the ground. Therefore, it is found in Figure 11d that the surface settlement caused by MJS pile construction can be basically controlled within the threshold range.

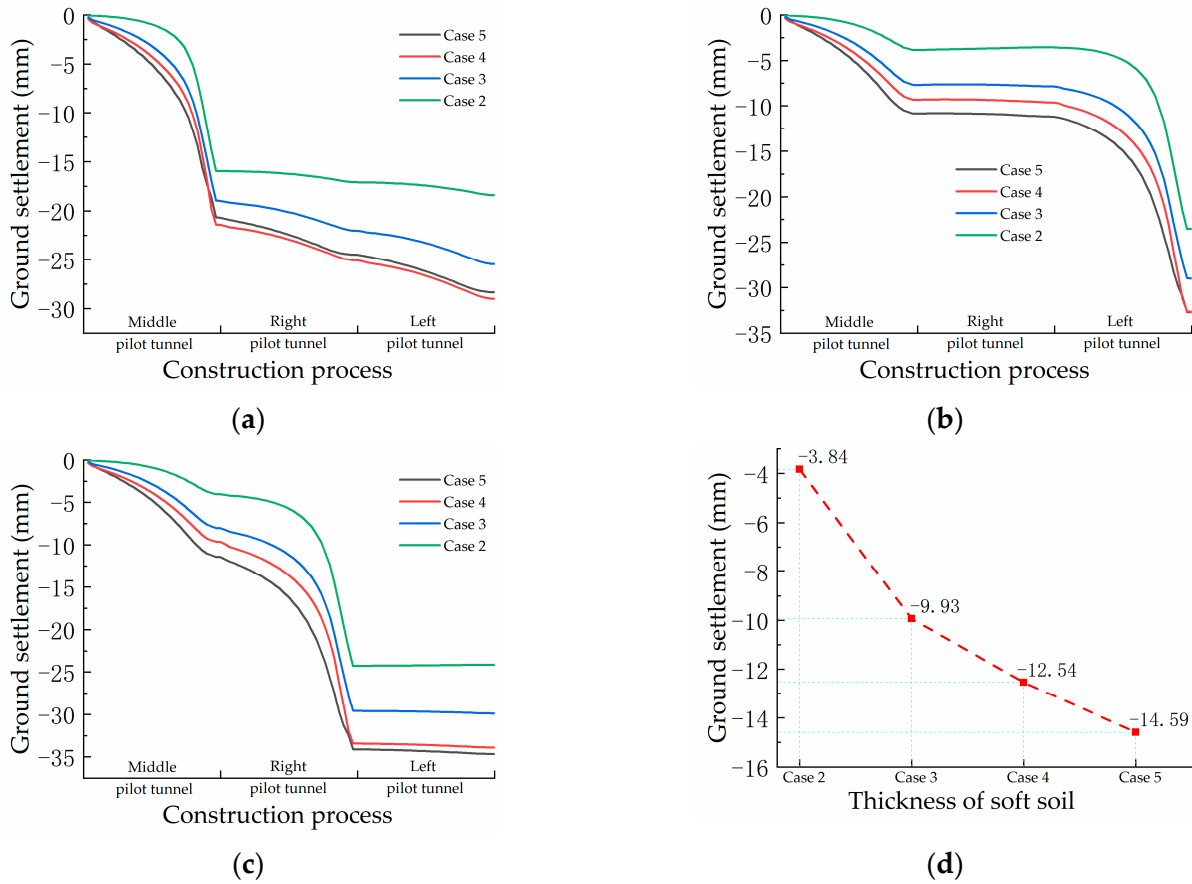


Figure 11. Reinforcement effect of MJS method pile: (a) Middle arch roof; (b) Right arch roof; (c) Left arch roof; (d) The settlement of MJS pile.

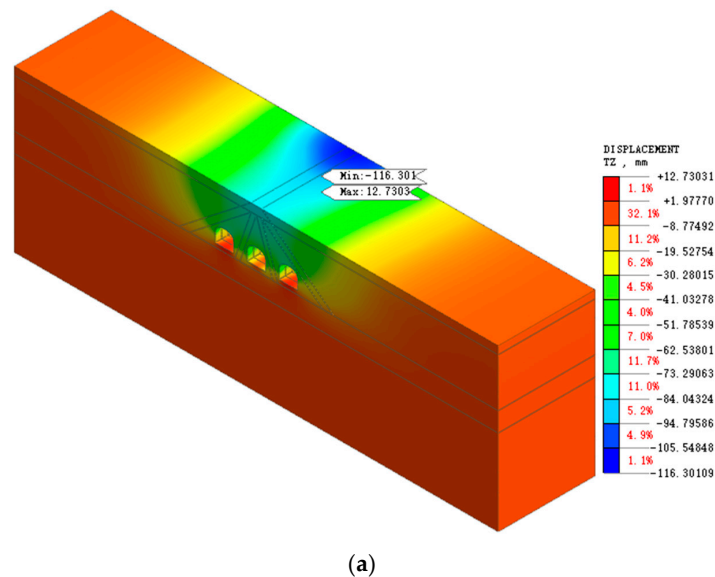
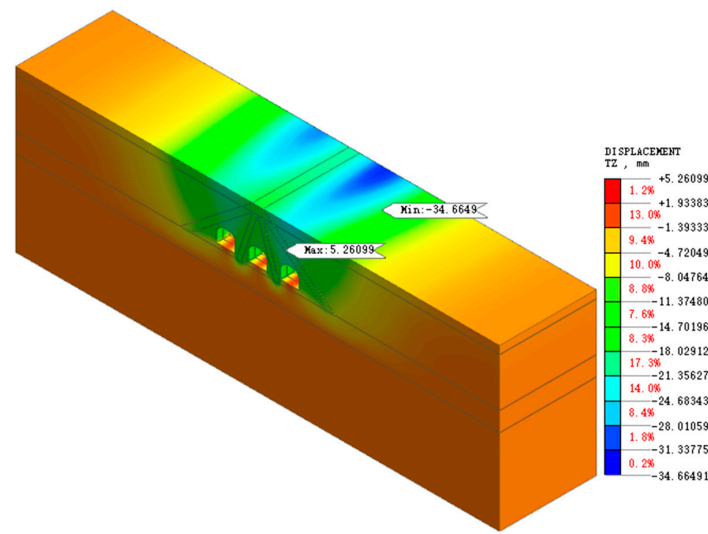


Figure 12. Cont.



(b)

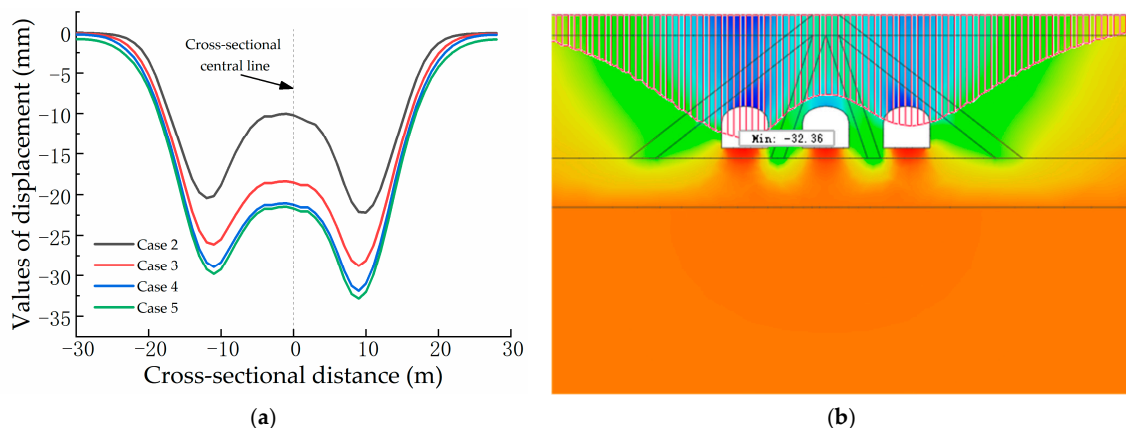
Figure 12. The vertical displacement cloud diagram of Case 5 before and after reinforcement: (a) Before reinforcement; (b) After reinforcement.

Table 2. MJS reinforcement settlement effect table.

Type	Unreinforced Settlement (mm)	Reinforcement Settlement (mm)	Decrement	Proportion
Case 2	48.57	24.16	24.41	50.30%
Case 3	65.40	29.89	35.51	54.30%
Case 4	79.64	33.90	45.74	57.40%
Case 5	116.3	34.66	81.64	70.20%

5.3.2. Lateral Surface Deformation

Under the reinforcement of the MJS pile, the change trend of the surface transverse deformation and the Peck curve are not the same. In Figure 13, in the case of reinforcement treatment, the settlement value of the center guide hole is lower than the settlement value of the two sides of the guide hole, which is different from the case without reinforcement treatment. This change is because there is a stable triangular area in the upper part of the center guide hole, and under the action of MJS piles on both sides, the weak silt is squeezed to increase the cohesion and friction angle of the soil. Under the action of two factors, the settlement of the center guide is greatly reduced, which is conducive to solving the problem of the excessive settlement rate of the center guide hole mentioned above.



(a)

(b)

Figure 13. Lateral deformation diagram after reinforcement: (a) Across settlement trough; (b) Across settlement cloud picture.

6. Conclusions

In this paper, three-dimensional finite element analysis was used to analyze the settlement law of different soft stratum thicknesses and the reinforcement effect of MJS piles. The idea of this paper was to first use the monitoring data and simulation data to verify the accuracy of the finite element simulation. After determining the rationality of the finite element model, without changing other parameters, the MJS construction method was used to reinforce the stratum by using the pile diameter of the MJS construction method. The following conclusions are drawn:

- (1) The greater the thickness of the plastic residual soil, the more unstable the ground surface caused by the excavation of the hole pile excavation method, the greater the settlement, and the greater the risk of collapse. The tunnel vault is located under the weak stratum, and the surface deformation is within the control value, so it does not need to be reinforced. The surface settlement of the whole tunnel section in the soft stratum is the fastest. The settlement is the largest, so the whole tunnel section in South China is in the thickness of plastic residual soil. It is necessary to go through the foundation reinforcement treatment before the next construction.
- (2) By comparing the monitoring value and the simulated value, it can be found that the surface deformation of the excavation of the pilot tunnel in the middle is obviously larger than that of the excavation of the pilot tunnel on both sides. After the primary stress release of the plastic residual soil, the amount of surface loss caused by the secondary stress release will be smaller. Therefore, by controlling the surface settlement of the central pilot tunnel, the total surface settlement can be controlled.
- (3) The MJS oblique jet grouting pile can reduce more than 50% of the deformation; the greater the thickness of the weak layer, the more obvious the effect, and eventually can reduce the settlement warning value. At the same time, in the formation process of the MJS pile, the plastic residual soil is squeezed, which improves the mechanical properties of the soil and is beneficial to controlling the deformation. Therefore, the oblique jet pile technology of the MJS construction method has a good reinforcing effect on the plastic residual soil.

Author Contributions: Conceptualization, J.L. (Jianbing Lv) and J.L. (Jianjun Lu); methodology, J.H. (Jingkai Huang); software, J.H. (Juan Huang) and X.G.; validation, J.L. (Jianjun Lu); formal analysis, J.L. (Jia Li); investigation, J.L. (Jianbing Lv); resources, J.H. (Juan Huang); data curation, J.L. (Jia Li) and J.H. (Jingkai Huang); writing—original draft preparation, J.L. (Jianjun Lu); writing—review and editing, J.L. (Jianbing Lv) and J.L. (Jianjun Lu). All authors have read and agreed to the published version of the manuscript.

Funding: Foundation of Outstanding Youth of Guangdong Province—Research on Bearing Mechanism and Stability of pile foundation in Karst Area based on static and dynamic loads and time-varying soil Characteristics, (Approval number: 2023B1515020061); Study on time-varying characteristics of stability of large-diameter steel pipe piles in calcareous sand strata in marine environment (Approval No.: 52278336).

Data Availability Statement: Not applicable.

Conflicts of Interest: The authors declare no conflict of interest.

References

1. Ajay, P.; Nagaraj, B.; Pillai, B.M.; Suthakorn, J.; Bradha, M. Intelligent ecofriendly transport management system based on IoT in urban areas. *Environ. Dev. Sustain.* **2022**. [[CrossRef](#)]
2. Guo, X.; Jiang, A. Study on the stability of a large-span subway station constructed by combining with the shaft and arch cover method. *Tunn. Undergr. Space Technol.* **2022**, *127*, 104582. [[CrossRef](#)]
3. Cao, X.; Schoner, J. The influence of light rail transit on transit use: An exploration of station area residents along the Hiawatha line in Minneapolis. *Transp. Res. Part A-Policy Pract.* **2014**, *59*, 134–143. [[CrossRef](#)]
4. Avunduk, E.; Copur, H. Effect of Clogging on EPB TBM Performance: A Case Study in Akfirat Waste Water Tunnel, Turkey. *Geotech. Geol. Eng.* **2019**, *37*, 4789–4801. [[CrossRef](#)]
5. Bernat, S.; Cambou, B. Soil-structure interaction in shield tunnelling in soft soil. *Comput. Geotech.* **1998**, *22*, 221–242. [[CrossRef](#)]

6. Gao, F.; Li, Z.F.; Yang, K.W.; Chen, Y.M.; Bian, X.C. Shield tunneling-induced disturbance in soft soil. *Transp. Geotech.* **2023**, *40*, 100971. [[CrossRef](#)]
7. Olsen, T.; Kasper, T.; de Wit, J. Immersed tunnels in soft soil conditions experience from the last 20 years. *Tunn. Undergr. Space Technol.* **2022**, *121*, 104315. [[CrossRef](#)]
8. Yu, L.; Zhang, D.; Fang, Q.; Cao, L.; Xu, T.; Li, Q. Surface settlement of subway station construction using pile-beam-arch approach. *Tunn. Undergr. Space Technol.* **2019**, *90*, 340–356. [[CrossRef](#)]
9. Nguyen, X.L.; Wu, L.; Nguyen, K.T.; Bui, Q.A. Application research of high pressure jet grouting pile in an underground engineering in Vietnam. *Arch. Civ. Eng.* **2020**, *66*, 575–593. [[CrossRef](#)]
10. Modoni, G.; Bzowka, J. Analysis of Foundations Reinforced with Jet Grouting. *J. Geotech. Geoenviron. Eng.* **2012**, *138*, 1442–1454. [[CrossRef](#)]
11. Burke, G.K. Jet grouting systems: Advantages and disadvantages. In Proceedings of the GeoSupport Conference 2004, Orlando, FL, USA, 29 December 2004; pp. 875–886. [[CrossRef](#)]
12. Nakashima, K.; Kashima, T.; Sakuma, T.; Murakami, T. Applications of MJS Method (Metro Jet System)—All-around Type Reinforcing and Consolidating Method in the Ground. Available online: https://jglobal.jst.go.jp/detail?JGLOBAL_ID=201002196477516747 (accessed on 1 January 1996).
13. Yang, Y.B.; Li, J.S.; Liu, C.; Ma, J.J.; Zheng, S.; Chen, W. Influence of deep excavation on adjacent bridge piles considering underlying karst cavern: A case history and numerical investigation. *Acta Geotech.* **2022**, *17*, 545–562. [[CrossRef](#)]
14. Liu, X.; Liu, Y.; Qu, W.; Tu, Y. Internal force calculation and supporting parameters sensitivity analysis of side piles in the subway station excavated by Pile-Beam-Arch method. *Tunn. Undergr. Space Technol.* **2016**, *56*, 186–201. [[CrossRef](#)]
15. Chen, R.P.; Lin, X.T.; Kang, X.; Zhong, Z.Q.; Liu, Y.; Zhang, P.; Wu, H.N. Deformation and stress characteristics of existing twin tunnels induced by close-distance EPBS under-crossing. *Tunn. Undergr. Space Technol.* **2018**, *82*, 468–481. [[CrossRef](#)]
16. Oda, K.; Kaji, S.; Nakajima, K.; Nakagawa, K. Horizontal Jet-mixing method for ground Improvement. In *Soft Soil Engineering*; Routledge: London, UK, 25 October 2017; pp. 483–488. [[CrossRef](#)]
17. Fan, H.; Xu, Q.; Lai, J.; Liu, T.; Zhu, Z.; Zhu, Y.; Gao, X. Stability of the loess tunnel foundation reinforced by jet grouting piles and the influence of reinforcement parameters. *Transp. Geotech.* **2023**, *40*, 100965. [[CrossRef](#)]
18. Li, Z.; Lv, J.; Xie, X.; Fu, H.; Huang, J.; Li, Z. Mechanical characteristics of structures and ground deformation caused by shield tunneling under-passing highways in complex geological conditions based on the MJS method. *Appl. Sci.* **2021**, *11*, 9323. [[CrossRef](#)]
19. Cherlo, M.A.; Hashemolhosseini, H.; Cheraghi, M.; Mahdevari, S. Feasibility evaluation for excavation of Naghshe Jahan Square subway station by underground methods. *J. Rock Mech. Geotech. Eng.* **2013**, *5*, 452–459. [[CrossRef](#)]
20. Nguyen, V.-Q.; Lee, Y.-G.; Park, D. Seismic damage evaluation of double-box metro tunnel accounting for soil stiffness using three-dimensional finite element analysis. *Structures* **2023**, *50*, 1584–1597. [[CrossRef](#)]
21. Keskin, İ.; Ahmed, M.Y.; Taher, N.R.; Gör, M.; Abdulsamad, B.Z. An evaluation on effects of surface explosion on underground tunnel; availability of ABAQUS Finite element method. *Tunn. Undergr. Space Technol.* **2022**, *120*, 104306. [[CrossRef](#)]
22. Hernandez, Y.Z.; Farfan, A.D.; de Assis, A.P. Three-dimensional analysis of excavation face stability of shallow tunnels. *Tunn. Undergr. Space Technol.* **2019**, *92*, 103062. [[CrossRef](#)]
23. Klotoé, C.H.; Bourgeois, E. Three dimensional finite element analysis of the influence of the umbrella arch on the settlements induced by shallow tunneling. *Comput. Geotech.* **2019**, *110*, 114–121. [[CrossRef](#)]
24. Heidari, M.; El Naggar, M.H. Design guideline for extended pile shaft incorporating nonlinear pile-soil interaction. *Ocean Eng.* **2022**, *243*, 109371. [[CrossRef](#)]
25. Bao, X.; Wu, S.; Liu, Z.; Su, D.; Chen, X. Study on the nonlinear behavior of soil–pile interaction in liquefiable soil using 3D numerical method. *Ocean Eng.* **2022**, *258*, 111807. [[CrossRef](#)]
26. GB 50911-2013; Technical Specification for Monitoring of Urban Rail Transit Projects. Ministry of Housing and Urban-Rural Development: Beijing, China, 2013.
27. Flora, A.; Modoni, G.; Lirer, S.; Croce, P. The diameter of single, double and triple fluid jet grouting columns: Prediction method and field trial results. *Geotechnique* **2013**, *63*, 934–945. [[CrossRef](#)]
28. Zhang, Y.; Zou, Q. A prediction model for the slot depth of high pressure water jet. *Results Phys.* **2018**, *11*, 1105–1109. [[CrossRef](#)]
29. Ho, C.E. Turbulent Fluid Jet Excavation in Cohesive Soil: With Particular Application to Jet Grouting. Doctoral Dissertation, Massachusetts Institute of Technology, Cambridge, MA, USA, 1 June 2005.
30. Shen, S.-L.; Wang, Z.-F.; Yang, J.; Ho, C.-E. Generalized Approach for Prediction of Jet Grout Column Diameter. *J. Geotech. Geoenviron. Eng.* **2013**, *139*, 2060–2069. [[CrossRef](#)]
31. Greenwood, D.A. Theoretical modelling of jet grouting—Discussion. *Geotechnique* **2008**, *58*, 533–535. [[CrossRef](#)]
32. Lv, J.B.; Lu, J.J.; Wu, H. Study on the Mechanical Characteristics and Ground Surface Settlement Influence of the Rise-Span Ratio of the Pile-Beam-Arch Method. *Appl. Sci.* **2023**, *13*, 5678. [[CrossRef](#)]

Disclaimer/Publisher’s Note: The statements, opinions and data contained in all publications are solely those of the individual author(s) and contributor(s) and not of MDPI and/or the editor(s). MDPI and/or the editor(s) disclaim responsibility for any injury to people or property resulting from any ideas, methods, instructions or products referred to in the content.